NASA TECHNICAL NOTE

NASA TN D-4915

C.1

NASA TN D-4915

LUNAR SURFACE TRANSMISSION LOSS FOR THE APOLLO ASTRONAUT

by Jefferson F. Lindsey III

Manned Spacecraft Center
Houston, Texas

NATIONAL AERONAUTICS AND SPACE ADMINISTRATION • WASHINGTON, D. C. • DECEMBER 1968

NASA TN D-4915

LUNAR SURFACE TRANSMISSION LOSS FOR THE APOLLO ASTRONAUT

By Jefferson F. Lindsey III

Manned Spacecraft Center
Houston, Texas

NATIONAL AERONAUTICS AND SPACE ADMINISTRATION

For sale by the Clearinghouse for Federal Scientific and Technical Information
Springfield, Virginia 22151 – CFSTI price $3.00

ABSTRACT

Radio-wave propagation theory is reviewed with emphasis on point-to-point communications on the lunar surface. The geometric optics solutions for both a plane surface and a spherical surface are presented. The transmission loss is found to slope at 40 dB/decade of distance at the longer distances for which the path difference between the direct and the reflected wave is less than one-half wavelength. The Bremmer series for radio-wave diffraction solution is presented for calculation of the transmission loss near the line of sight when the geometric optics solution does not apply. In addition to smooth-surface effects, the roughness effects of knife-edge diffraction and of small hills are used to obtain a combined-effects transmission loss plot. Finally, measured data are presented which confirm that the maximum astronaut-to-lunar-module range will be at least 8200 feet and that the maximum astronaut-to-astronaut range will be at least 6000 feet.

LUNAR SURFACE TRANSMISSION LOSS

FOR THE APOLLO ASTRONAUT

By Jefferson F. Lindsey III
Manned Spacecraft Center

SUMMARY

Radio-wave propagation theory is reviewed with emphasis on point-to-point communications on the lunar surface. The geometric optics solutions for both a plane surface and a spherical surface are presented. The transmission loss is found to slope at 40 dB/decade of distance at the longer distances for which the path difference between the direct and the reflected wave is less than one-half wavelength. The Bremmer series for radio-wave diffraction solution is presented for calculation of the transmission loss near the line of sight when the geometric optics solution does not apply. In addition to smooth-surface effects, the roughness effects of knife-edge diffraction and of small hills are used to obtain a combined-effects transmission loss plot. Finally, measured data are presented which show that the maximum astronaut-to-astronaut range will be at least 6000 feet and that the maximum astronaut-to-lunar-module range will be at least 8200 feet.

INTRODUCTION

The transmission loss for point-to-point communications on the lunar surface is evaluated. The astronaut-to-astronaut and astronaut-to-lunar-module links are considered at the Apollo astronaut transmit frequencies of 279.0 and 259.7 megahertz. The transmission loss is used as part of a circuit margin analysis to determine the Apollo astronaut's maximum range. Modulation degradation caused by multipath loss is not considered in this report.

The geometric optics and Bremmer series solutions are presented for a smooth-surface model; then, rough-surface effects are incorporated into the geometric optics solution to yield the combined effects. The smooth-surface model is finally compared with measured data taken at the NASA Manned Spacecraft Center.

Smooth-surface effects have been rigorously determined by Bremmer (ref. 1) with a derivation for the received electric field in the presence of a large dielectric body such as the earth or the moon. Applications of the Bremmer series and the geometric optics solutions are discussed in reference 2 by Burrows. Rough-surface effects are discussed in reference 3 by Beckmann and Spizzichino and in reference 4 by Deygout.

SYMBOLS

a	radius of a spherical body
c	speed of light
D	divergence factor
d	distance along surface from base of first antenna to base of second antenna
d_1	distance from base of first antenna to point of reflection
d_2	distance from point of reflection to base of second antenna
$\vec{E}_o$	received free-space electric field
$\vec{E}_r$	received electric field
$\vec{E}_t$	transmitting electric field
f	frequency
$f_n(h)$	height-gain function
h_1, h_2	antenna height
h_1', h_2'	equivalent antenna height
k	index of refraction
L	transmission loss
L_B	Bremmer loss factor
L_{ed}	edge diffraction loss
L_{mp}	multipath loss factor
L_o	free-space transmission loss
L_t	total transmission loss

n summation index

$\vec{R}$ complex reflection (Fresnel) coefficient

$\vec{R}_H$ Fresnel reflection coefficient with horizontal polarization

$\vec{R}_s$ rough-surface reflection coefficient

$\vec{R}_v$ Fresnel reflection coefficient with vertical polarization

r direct path or distance between phase centers of antennas

r_1 distance from first antenna to point of reflection

r_2 distance from point of reflection to second antenna

γ grazing angle (angle of incidence equal to angle of reflection)

γ' equivalent grazing angle

δ path difference between direct and reflected waves

δ' effective path difference between direct and reflected waves

δ'' ground parameter

$\vec{\epsilon}_c$ complex dielectric constant

ϵ_r real dielectric constant

ζ distance factor

λ wavelength

ρ_s scattering coefficient

σ conductivity

σ_h edge diffraction height

σ_{rms} root-mean-square (rms) roughness height

τ_n mode number, $n = 1, 2, 3, \ldots$

Φ reflection-coefficient phase angle

ϕ reflected-wave phase lag

ϕ' modified reflected-wave phase lag with curvature effects

An arrow above a symbol means that the symbol is a phasor (complex number).

SMOOTH-SURFACE EFFECTS

Before showing the smooth-surface effects on transmission loss, the free-space loss L_o is defined in equation (1) as the ratio of the power received to the power transmitted, with two isotropic antennas. The free-space loss is not a dissipative loss, but rather a measure of the dispersion of the spherical wave.

$$L_o = \left(\frac{\vec{E}_o}{\vec{E}_t}\right)^2 = \frac{\lambda^2}{(4\pi d)^2} = \frac{c^2}{(4\pi d f)^2} \tag{1}$$

where $\lambda^2/4\pi$ is the effective area of an isotropic antenna, and $4\pi d^2$ is the surface area of a sphere at a distance d. The free-space loss is plotted in figure 1 for the astronaut transmit frequency of 259.7 megahertz. The following observations relating the free-space loss with wavelength and distance may be inferred from equation (1):

1. At a distance of one wavelength ($d = \lambda$), the free-space loss is $(1/4\pi)^2$ or -22 decibels.

2. If the distance is increased by 10 feet, the signal decreases by 20 decibels, to result in a -20-dB/decade slope $\left(1/d^2\right)$.

In figure 1, the transmission loss for the 259.7-megahertz frequency is -22 decibels at 3.8 feet (one wavelength). At 38 feet, the loss is -42 decibels, and at 380 feet, the loss is -62 decibels. The free-space loss at the 279.0-megahertz frequency is 0.62 decibel greater than that at the 259.7-megahertz frequency.

Geometric Optics for a Plane Surface

The free-space loss is used to calculate the maximum range for land-to-air communications; however, when both the receiving and the transmitting antennas are located near a large body such as the earth or the moon, the free-space loss must be modified to include surface effects. Such a modification is obtained by using the geometric optics model for a plane surface (fig. 2). The modified received electric field $\vec{E}_r$ is composed of a direct field $\vec{E}_o$ that would be received under free-space conditions, plus a reflected field that comes from the surface. The geometric optics equation for a plane dielectric surface is

$$\vec{E}_r = \vec{E}_o + \vec{E}_o |\vec{R}| \left(\frac{r}{r_1 + r_2}\right) e^{j\phi} \tag{2}$$

where $\phi = \Phi + \frac{2\pi}{\lambda}\delta$; $\vec{R}$ is the complex reflection (Fresnel) coefficient; ϕ is the phase lag obtained from the path difference and the reflection coefficient; δ is the path difference, which is always negative and is defined by $r - (r_1 + r_2)$; Φ is the phase angle of the reflection coefficient and is always negative for a phase lag; and $r/(r_1 + r_2)$ is the amplitude reduction that results from the longer path length of the reflected field.

Using Euler's identity and the double-angle formula, equation (2) may be rewritten and expressed as the multipath loss factor

$$L_{mp} = \left(\frac{\vec{E}_r}{\vec{E}_o}\right)^2 = \left[1 - |\vec{R}| \left(\frac{r}{r_1 + r_2}\right)\right]^2 + 4|\vec{R}| \left(\frac{r}{r_1 + r_2}\right) \cos^2 \frac{\phi}{2} \tag{3}$$

The total transmission loss may be obtained by multiplying the free-space loss and multipath loss factor such that

$$L_t = L_o L_{mp} = \left(\frac{\vec{E}_r}{\vec{E}_t}\right)^2 \tag{4}$$

or in decibels

$$10 \log_{10} L_t = 10 \log_{10} L_o + 10 \log_{10} L_{mp} \tag{5}$$

Using decibel notation, the free-space loss is added to the multipath loss (or gain).

The Fresnel reflection coefficient from equation (3) may be expressed as (ref. 2)

$$\vec{R}_V = \frac{\vec{\epsilon}_c \sin\gamma - \sqrt{\vec{\epsilon}_c - \cos^2\gamma}}{\vec{\epsilon}_c \sin\gamma + \sqrt{\vec{\epsilon}_c - \cos^2\gamma}} = \left|\vec{R}_V\right| e^{j\Phi} \tag{6}$$

for vertical polarization, and may be expressed as

$$\vec{R}_H = \frac{\sin\gamma - \sqrt{\vec{\epsilon}_c - \cos^2\gamma}}{\sin\gamma + \sqrt{\vec{\epsilon}_c - \cos^2\gamma}} = \left|\vec{R}_H\right| e^{j\Phi} \tag{7}$$

for horizontal polarization. In equations (6) and (7), $\vec{\epsilon}_c$ is the complex dielectric constant given by

$$\vec{\epsilon}_c = \epsilon_r - j60\sigma\lambda \tag{8}$$

where ϵ_r is the real dielectric constant, σ is the conductivity, and λ is the wavelength. The reflection coefficient versus grazing angle is plotted in figure 3 for dielectric constants of 1.4 and 4.0, with conductivities of 10^{-5} mhos/m and 10^{-3} mhos/m and with vertical polarization. At near-grazing angles or long distances, the reflection coefficient approaches -1 (or $|\vec{R}| = 1$ and $\Phi = -180°$). Using the previous approximation and assuming the direct and reflected paths are equal (that is, $r/(r_1 + r_2) \approx 1$), the multipath equation may be simplified to

$$L_{mp} = 4 \sin^2\left(\frac{1}{2} \frac{2\pi}{\lambda} \delta\right) \tag{9}$$

where the path difference is

$$\delta = \left[d^2 + (h_1 - h_2)^2\right]^{1/2} - \left[d^2 + (h_1 + h_2)^2\right]^{1/2} \tag{10}$$

For longer distances, the antenna heights h_1 and h_2 are much less than the distance d, and equation (10) becomes

$$\delta = -\frac{2h_1h_2}{d} \tag{11}$$

Using equation (11) in equation (9), the long-distance multipath approximation becomes

$$L_{mp} = 4 \sin^2\left(\frac{2\pi}{\lambda}\frac{h_1h_2}{d}\right) \tag{12}$$

In equation (12), the multipath loss varies at the rate of -20 dB/decade of distance $\left(1/d^2\right)$ when the path difference is less than 20°; thus, the total transmission loss L_t varies at the rate of -40 dB/decade of distance $\left(1/d^4\right)$.

The total phase lag of the reflected wave is given as

$$\phi = \Phi + \frac{2\pi}{\lambda}\delta \tag{13}$$

The phase contributions from the reflection coefficient and the path difference are both negative, corresponding to a lag in the reflected wave.

Geometric Optics for a Curved Surface

In figure 4, the effect of changing the geometry from that of a plane-surface model to that of a curved-surface model is shown. A new expression for the received field may be written as follows:

$$\overline{E}_r = \overline{E}_o + \overline{E}_o D|\overline{R}|\left(\frac{r}{r_1 + r_2}\right)e^{j\phi'} \tag{14}$$

The divergence factor D ranges from 1 at short distances to zero at the limit of the line of sight, and the reflected field is reduced to zero at the line of sight. The divergence factor is (ref. 5)

$$D = \left[1 + \frac{2r_1r_2d}{ka\left(r_1 + r_2\right)\left(h_1' + h_2'\right)}\right]^{-1/2} \tag{15}$$

where a is the body radius and k is the index of refraction of the atmosphere, which is assumed to be 1 for the moon. The modified phase lag ϕ' is obtained by using the equivalent antenna heights h_1' and h_2' (fig. 4).

$$h_1' = h_1 - \frac{d_1^{\,2}}{2ka} \tag{16}$$

$$h_2' = h_2 - \frac{d_2^{\,2}}{2ka} \tag{17}$$

The equivalent antenna heights are essentially unaffected at shorter distances; however, as the line of sight is approached, the equivalent heights approach zero. The effective phase lag, which is modified by the curvature, is now

$$\phi' = \Phi + \frac{2\pi}{\lambda}\delta'$$

or

$$\phi' = \Phi - \frac{2\pi}{\lambda}\left(\frac{2h_1'h_2'}{d}\right) \tag{18}$$

The grazing angle used to determine Φ must also be modified such that

$$\gamma' = \sin^{-1}\left(\frac{h_1' + h_2'}{d}\right) \tag{19}$$

The multipath expression with the curved-surface model becomes

$$L_{mp} = \left[1 - D|\vec{R}|\left(\frac{r}{r_1 + r_2}\right)\right]^2 + 4D|\vec{R}|\left(\frac{r}{r_1 + r_2}\right)\cos^2\left(\frac{1}{2}\phi'\right) \tag{20}$$

At shorter distances, the curved-surface model gives results that are similar to the results for the plane-surface model; however, as the line of sight is approached, the divergence approaches zero, and the received field becomes the same as free space. If the divergence is neglected, then cancellation of the direct and reflected fields takes place, and the received field approaches zero.

Bremmer Series

At distances near the line of sight, the geometric optics solutions do not apply, and the effect of diffraction needs to be considered. The diffraction around a smooth sphere is described by the Bremmer series solution as follows (ref. 2):

$$|\vec{E}_r| = 2|\vec{E}_o| (2\pi\zeta)^{1/2}\left|\sum_{n=1}^{\infty} \frac{e^{-j\tau_n\zeta}}{\delta'' + 2\tau_n} f_n(h_1) f_n(h_2)\right| \tag{21}$$

The Bremmer loss factor L_B may be compared with the power received over free space as follows:

$$L_B = \left(\frac{\vec{E}_r}{\vec{E}_o}\right)^2 = 8\pi\zeta\left|\sum_{n=1}^{\infty} \frac{e^{-j\tau_n\zeta}}{\delta'' + 2\tau_n} f_n(h_1) f_n(h_2)\right|^2 \tag{22}$$

where δ'' is the ground parameter, ζ is the distance factor, τ_n is the mode number, and $f_n(h)$ is the height-gain function. The following are the parameters of equation (22):

1. The ground parameter is

$$\delta'' = \left(\frac{2\pi ka}{\lambda}\right)^{2/3}\left(\frac{\vec{\epsilon}_c - 1}{\vec{\epsilon}_c^{\,2}}\right) \tag{23}$$

for vertical polarization, and

$$\delta'' = \left(\frac{2\pi ka}{\lambda}\right)^{2/3}\left(\bar{\epsilon}_c - 1\right) \tag{24}$$

for horizontal polarization, where ka is the effective radius.

2. The distance factor is

$$\zeta = \left(\frac{2\pi}{\lambda(ka)^2}\right)^{1/3} d \tag{25}$$

3. The mode numbers are presented in the following table in which $\delta'' = 0$ is used for the perfect-conductivity cases and $\delta'' \to \infty$ is used for dielectric cases at short wavelengths (ref. 2).

	$\delta'' = 0$	$\delta'' \to \infty$
τ_1	$0.885e^{-j\pi/3}$	$1.856e^{-j\pi/3}$
τ_2	$2.577e^{-j\pi/3}$	$3.245e^{-j\pi/3}$
τ_3	$3.824e^{-j\pi/3}$	$4.382e^{-j\pi/3}$
$\tau_n, n \geq 4$	$\frac{1}{2}\left[3\pi\left(n + \frac{3}{4}\right)\right]^{2/3} e^{-j\pi/3}$	$\frac{1}{2}\left[3\pi\left(n + \frac{1}{4}\right)\right]^{2/3} e^{-j\pi/3}$

4. The height-gain function $\left(\text{for } h < 30\lambda^{2/3}\right)$ is

$$f(h) = 1 + j\left(\frac{2\pi h}{\lambda}\right)\left(\frac{\sqrt{\bar{\epsilon}_c - 1}}{\bar{\epsilon}_c}\right) \tag{26}$$

for vertical polarization, and

$$f(h) = 1 + j\left(\frac{2\pi h}{\lambda}\right)\sqrt{\bar{\epsilon}_c - 1} \tag{27}$$

for horizontal polarization. Equations (1), (20), and (22) for L_o, L_{mp}, and L_B, respectively, are plotted in figure 5 with the use of a computer program to show the transmission loss as a function of distance.

For the astronaut-to-lunar-module range (fig. 5(a)), the geometric optics solution and the first seven terms of the Bremmer series solution give essentially the same results for distances between 300 and 5000 feet. At distances of less than 5000 feet, the geometric optics solution may be applied, and at distances beyond 3000 feet, the Bremmer series solution may be applied. The dielectric-constant and conductivity variations do not have a significant effect on transmission loss at the maximum ranges at very high frequencies. At lower frequencies, the ground conductivity becomes much more important (refs. 6 to 8).

ROUGH-SURFACE EFFECTS

The smooth-surface transmission loss as described in the previous section may be used to make a reasonable estimation of the worst-case transmission loss on the surface of the moon; however, a more refined estimation may be obtained by considering the effects on roughness. The factors considered in this section are scattering, edge diffraction, and small-hill effects. In general, the transmission loss for a randomly rough surface tends to be less than the transmission loss for a smooth surface because of the breakup of the reflected wave by the surface roughness.

Scattering

Scattering modifies the reflection coefficient such that the rough-surface reflection coefficient may be expressed in terms of the rms roughness σ_{rms} and the effective grazing angle γ', as follows (ref. 5):

$$\left|\vec{R}_s\right| = \rho_s \left|\vec{R}\right| \tag{28}$$

where

$$\left\langle \left|\rho_s\right|^2 \right\rangle = \exp\left(-\frac{4\pi\sigma_{rms}}{\lambda}\sin\gamma'\right)^2 \tag{29}$$

which is the scattering coefficient.

For the relatively low astronaut and lunar-module antenna heights, the rms roughness has to be much larger than the antenna heights in order to have a scattering coefficient significantly less than 1 at distances greater than 250 feet. As a result, the normal scattering does not occur, but rather a multiple edge diffraction phenomenon takes place. If the Rayleigh roughness criterion is applied for the astronaut-to-lunar-module link, it is found that an rms roughness of 170 feet is required at a distance of 10 000 feet. At 1000 feet, the rms roughness is 17 feet. However, in either case, the astronaut antenna at a height of 6 feet would not have a clear line-of-sight path, and multiple knife-edge diffraction would occur.

Knife-Edge Diffraction

If the roughness is sufficiently large to block the line-of-sight path, the radio wave will propagate over the edges of the roughness. For the case when a steep hill, a rock, or a ridge is located between the two astronauts or between the astronaut and the lunar module, the edge diffraction loss may be expressed in decibels as (ref. 4)

$$10 \log_{10} L_{ed} = -20 \log_{10} \left(\frac{\sigma_h}{\sqrt{\frac{\lambda d_1 d_2}{d_1 + d_2}}} \right) - 16 \tag{30}$$

From figure 6(a), it is seen that σ_h is the height of the knife edge, and d_1 and d_2 are the distances along the surface to the knife edge. Equation (25) is valid when $\sigma_h > \sqrt{\frac{\lambda d_1 d_2}{d_1 + d_2}}$ and $\lambda \ll \sigma_h < d_1/10$ or $\lambda \ll \sigma_h < d_2/10$. The knife-edge diffraction is plotted in figure 6(b) for obstacle heights ranging between 10 and 400 feet for the astronaut-to-lunar-module link. In figure 6(b), the transmission loss is not as great as in the free-space case because the multipath cancellation does not take place. The standard edge diffraction equation does not apply when the rough edge is close to either the astronaut or the lunar module. In this case, losses greater than smooth-surface losses may occur. The calculation of this loss is not discussed in this report; however, it is known to extend to 50 decibels (ref. 4).

Small-Hill Effect

The small-hill effect is considered by changing the radius of the moon from 1738 to 173.8 kilometers and plotting the transmission loss in figure 7 for the astronaut-to-lunar-module link. The effect of changing the radius is not significant, except near and beyond the line of sight. At distances beyond 5000 feet, the small-hill loss begins to limit the astronaut's range from the lunar module. The Bremmer series solution is used to determine the loss near the line of sight.

COMBINED EFFECTS — MEASUREMENTS

The combined effects for the smooth curved-surface model and the roughness effects are shown in figure 8 for the astronaut-to-lunar-module link. The transmission loss has a wide range of values with all effects considered. The maximum range is achieved when the free-space loss occurs and the minimum range corresponds to the smooth-surface loss. The probability of achieving a particular maximum range is a function of the electrical surface and its roughness. For a smooth surface, the transmission loss will fall close to the values predicted in the smooth-surface model. As roughness effects are encountered, the astronaut range may be increased by as much as 10 over the smooth-surface conditions. It is doubtful that the conditions will be proper for this increase to occur.

In order to verify the theoretical equations of this paper, extensive measurements were taken to determine practical values for the transmission loss between two Apollo astronauts and between an astronaut and the lunar module. Data for the astronaut standing, bending over, and lying face down on the ground were taken in the vicinity of the antenna range at building 14 of the NASA Manned Spacecraft Center. Four orientations were used to include the effects of astronaut antenna pattern in the transmission loss curves.

The test setup and results of the data are shown in figures 9 to 11. The transmission loss is no greater than the theoretical smooth-surface values. At the range of 7000 feet, the astronaut stood on a 6-foot hill and also stood in a 6-foot gully. Even in the 6-foot gully, the loss was no greater than that predicted by the smooth-surface model. As the astronaut bent over and lay down, the losses of up to 25 decibels over the standing position occurred; however, for most of the time the additional loss was on the order of 12 decibels. The transmission loss in figures 10 and 11 includes the variational effects on the antenna pattern, and data points are taken for four positions.

CONCLUSIONS

The results of the theoretical study and the measured data show that the roughness could easily double the maximum range, which is predicted on the basis of a smooth-surface model. For smooth-surface conditions with the newest astronaut transmitter of 0. 5-watt output and 119-decibel loss between antenna terminals, the astronaut will be able to walk to a distance of 8200 feet and still communicate with the lunar module. In the bent-over or lying-down position, the range will normally be limited to 4100 feet. For the astronaut-to-astronaut link with the specified 128-decibel loss between antenna terminals, the standing range is 6000 feet, and the lying-down or bending-over range will normally be limited to 3000 feet. With the effects of roughness on the lunar surface considered, these smooth-surface ranges could easily be doubled. If the maximum predicted range had been close to the limit of the line of sight, then the conclusion of doubling the range could not be reached since roughness effects are not important beyond the line-of-sight limit. The previously mentioned nominal ranges are based on antenna pattern and cable losses of 3 decibels for the astronaut portable life-support-system monopole antenna and 2 decibels for the lunar-module extravehicular-activity antenna. For a worst-case condition with an additional 6 decibels of loss added for antenna pattern effects, the astronaut-to-lunar-module range is reduced to 6300 feet, and the astronaut-to-astronaut range is reduced to 4500 feet. For the worst-case condition of one astronaut bending over or lying down, the astronaut-to-lunar-module range is reduced to 1950 feet, and the astronaut-to-astronaut range is reduced to 1400 feet. The conditions for the ranges utilize a 119-decibel loss between the antenna terminal of the back transmitter and the antenna terminal of the lunar-module receiver. Also, a 128-decibel loss is used between the antenna terminals of the two astronaut transceivers.

Manned Spacecraft Center
National Aeronautics and Space Administration
Houston, Texas, August 23, 1968
914-50-50-09-72

REFERENCES

1. Bremmer, H.: Terrestrial Radio Waves. Elsevier Publishing Co., 1949.

2. Burrows, C. R.: Radio Wave Propagation. Academic Press, Inc., 1949.

3. Beckmann, P.; and Spizzichino, A.: The Scattering of Electromagnetic Waves from Rough Surfaces. Macmillan Company, 1963.

4. Deygout, J.: Multiple Knife-Edge Diffraction of Microwaves. IEEE Trans. on Antennas and Propagation, vol. AP-14, July 1966, pp. 480-489.

5. Beckmann, P.: Shadowing of Random Rough Surfaces. IEEE Trans. on Antennas and Propagation, vol. AP-13, May 1965, pp. 384-388.

6. Vogler, L. E.: Point-to-Point Communication on the Moon. NBS Report 7239, Mar. 1962.

7. Vogler, L. E.: A Study of Lunar Surface Radio Communication. NBS Monograph 85, Sept. 14, 1964.

8. Norton, K. A.: The Calculation of Ground-Wave Field Intensity Over a Finitely Conducting Spherical Earth. Proc. of IRE, vol. 29, Dec. 1941, pp. 623-39.

BIBLIOGRAPHY

Bachynski, M. P.: Microwave Propagation Over Rough Surfaces. RCA Review, Vol. XX, June 1959, pp. 308-335.

Brockelman, R. A.; and Hagfors, T.: Note on the Effect of Shadowing on the Backscattering of Waves From a Random Rough Surface. IEEE Trans. on Antennas and Propagation, vol. AP-14, Sept. 1966, pp. 621-28.

Brown, G. H.; Epstein, J.; and Peterson, P. W.: Comparative Propagation Measurements; Television Transmitters at 67.25, 288, 510 and 910 Megacycles. RCA Review, Vol. IX, June 1948, pp. 177-201.

Bullington, K.: Reflection Coefficients of Irregular Terrain. Proc. of IRE, vol. 42, Aug. 1954, pp. 1258-1262.

Burrows, C. R.: The Effect of the Earth's Curvature on Ground-Wave Propagation. Proc. of IRE, vol. 29, Jan. 1941, pp. 16-24.

Burrows, C. R.: Ultra-Short-Wave Propagation in the Jungle. IEEE Trans. on Antennas and Propagation, vol. AP-14, May 1966, pp. 386-388.

Carlson, A. B.; and Waterman, A. T., Jr.: Microwave Propagation Over Mountain-Diffraction Paths. IEEE Trans. on Antennas and Propagation, vol. AP-14, July 1966, pp. 489-496.

Carter, P. S.: Circuit Relations in Radiating Systems and Applications to Antenna Problems. Proc. of IRE, vol. 20, June 1932, pp. 1004-41.

Egli, J. J.: Radio Propagation Above 40 MC Over Irregular Terrain. Proc. of IRE, vol. 45, Oct. 1957, pp. 1383-1391.

Hayre, H. S.: Roughness and Radar Return. Proc. of IRE, vol. 50, Feb. 1962, pp. 223-224.

Hayre, H. S.; and Moore, R. K.: Radar Back-Scatter Theories for Near-Vertical Incidence and Their Application to an Estimate of the Lunar Surface Roughness. New Mexico University Report EE-67, Jan. 1962.

Josephson, B.; and Blomquist, A.: The Influence of Moisture in the Ground, Temperature and Terrain on Ground Wave Propagation in the VHF-Band. IEEE Trans. on Antennas and Propagation, vol. AP-6, Apr. 1958, pp. 169-172.

Kraus, John: Antennas. 1st. Ed., McGraw-Hill Book Company, Inc., 1950.

Pettengill, G. H.: Measurements of Lunar Reflectivity Using the Millstone Radar. Proc. of IRE, vol. 48, May 1960, pp. 933-934.

Senior, T. B. A.; and Siegel, K. M.: A Theory of Radar Scattering by the Moon. J. of Res. of the NBS — D. Radio Propagation, vol. 64D, no. 3, May-June 1960, pp. 217-229.

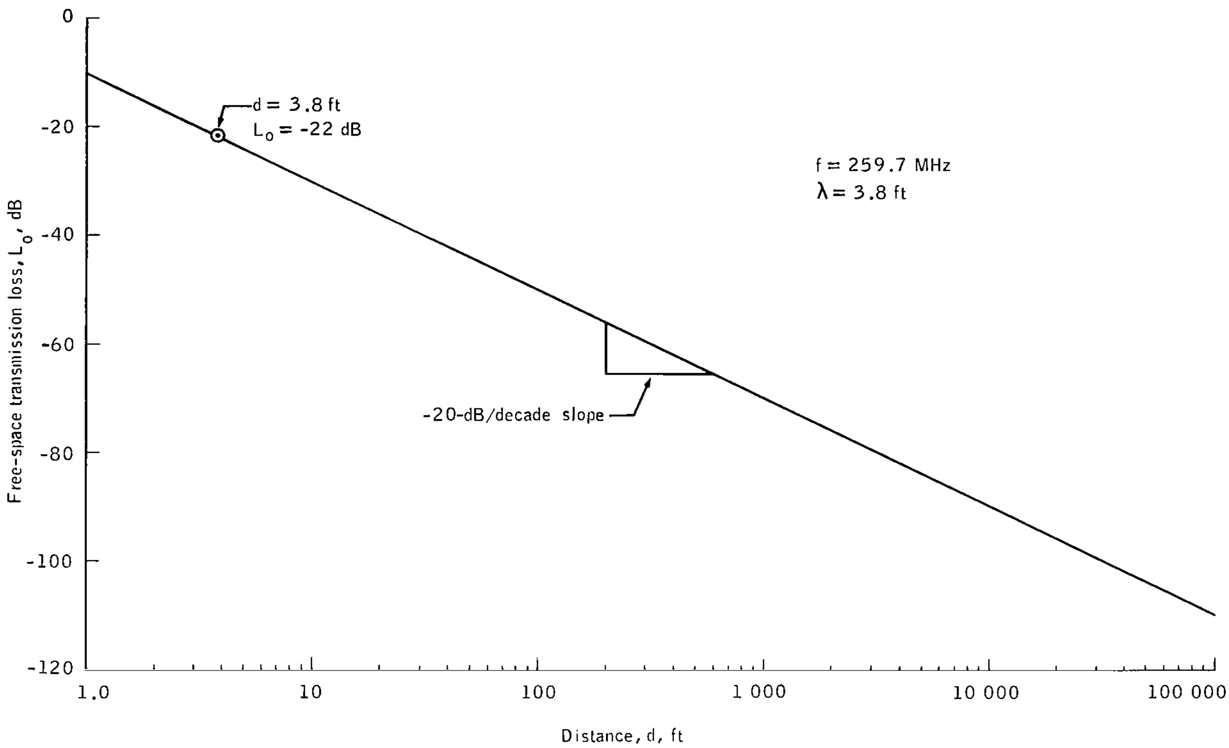

Figure 1. - Free-space loss.

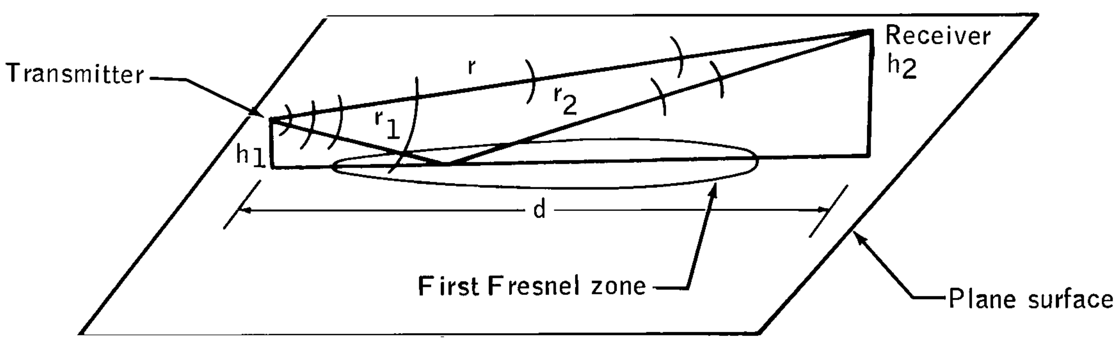

$$\left|\vec{E}_r\right| = \left|\vec{E}_o\right| + \left|\vec{E}_o\right|\left|\vec{R}\right| e^{j\Phi}\left(\frac{r}{r_1 + r_2}\right) e^{j\left(\frac{2\pi}{\lambda}\right)\delta}$$

Figure 2. - Plane-surface model.

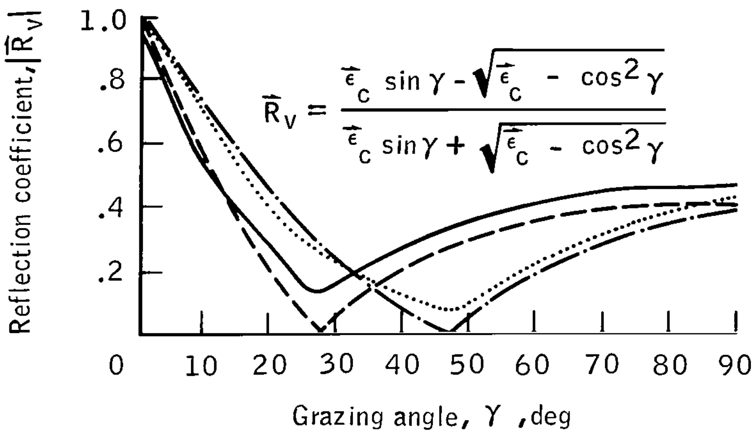

(a) Reflection coefficient versus grazing angle.

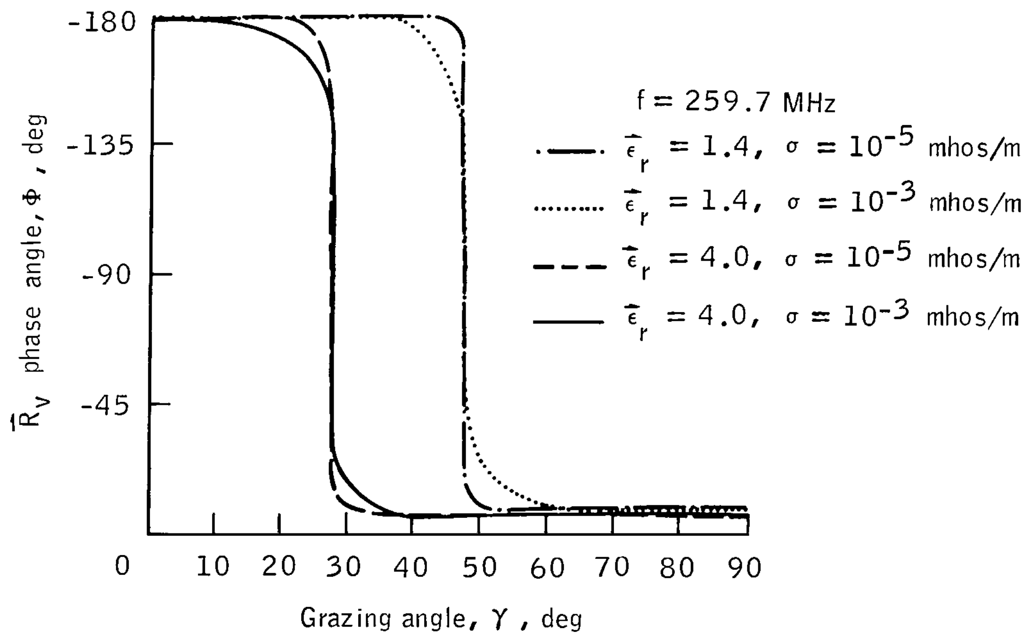

(b) Reflection-coefficient phase angle versus grazing angle.

Figure 3. - Reflection coefficient.

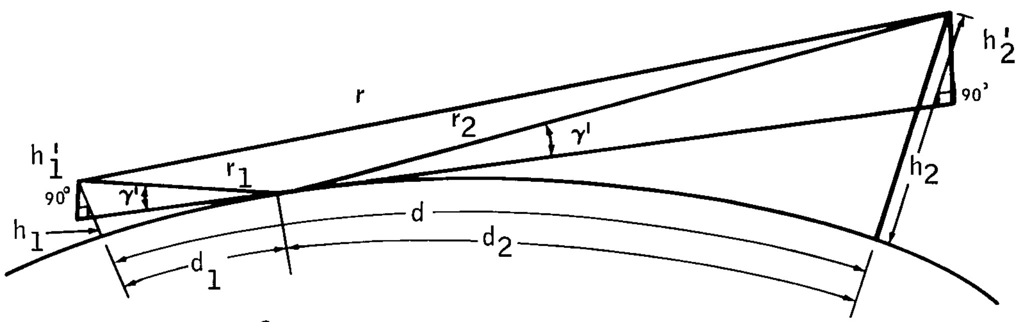

$$h_1' = h_1 - \frac{d_1^2}{2ka}$$

$$h_2' = h_2 - \frac{d_2^2}{2ka}$$

$$D = \left[1 + \frac{2r_1r_2d}{ka(r_1 + r_2)(h_1' + h_2')}\right]^{-1/2}$$

d, ft	h_1', ft	h_2', ft	D
0	6.0	24.0	1.00
5 000	5.9	22.4	.91
10 000	3.7	17.3	.45
24 700	0	0	~0

Figure 4. - Curved-surface model.

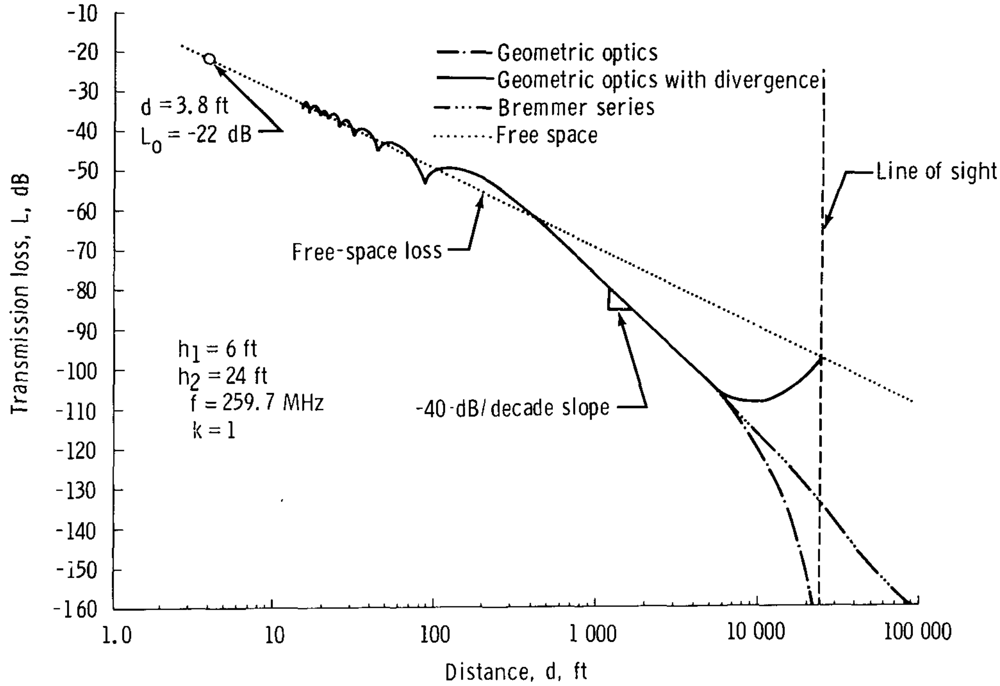

(a) Astronaut-to-lunar-module transmission loss.

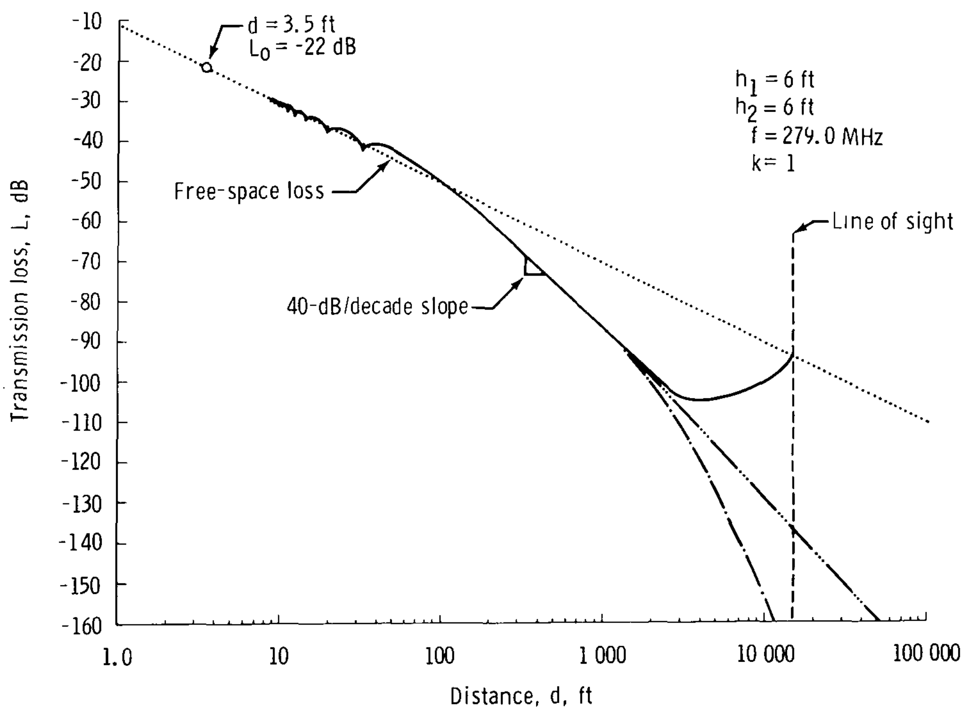

(b) Astronaut-to-astronaut transmission loss.

Figure 5. - Transmission loss as a function of distance.

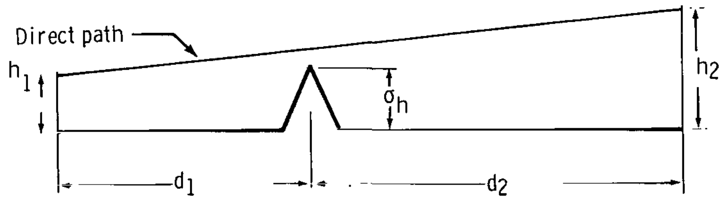

(a) Knife-edge diffraction model.

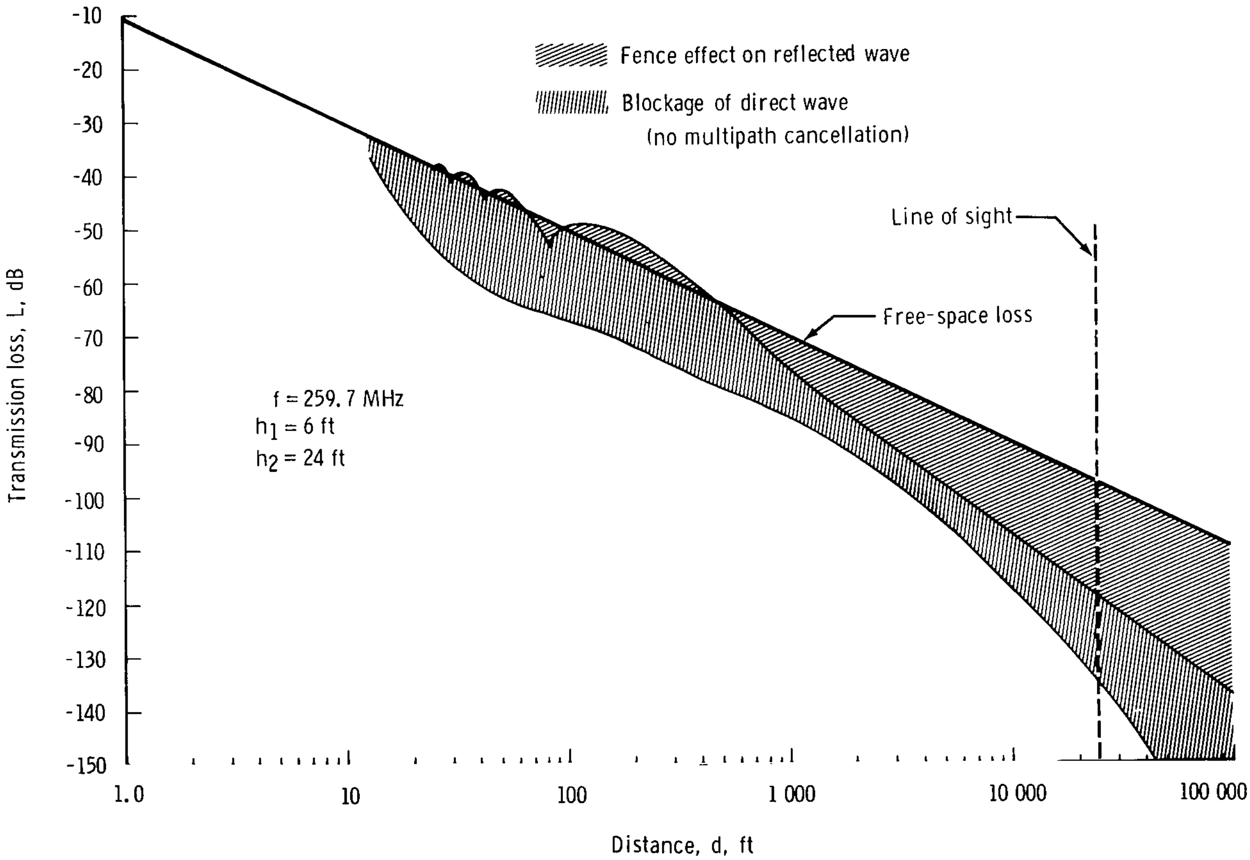

(b) Knife-edge diffraction for obstacle heights ranging from 10 to 400 feet.

Figure 6. - Knife-edge diffraction effects.

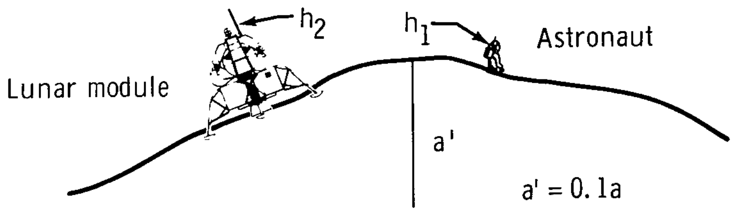

(a) Small-hill model.

Line of sight $= \sqrt{2a'h_1} + \sqrt{2a'h_2}$

a, km	Line of sight, ft
1738.0	24 800
173.8	7 500

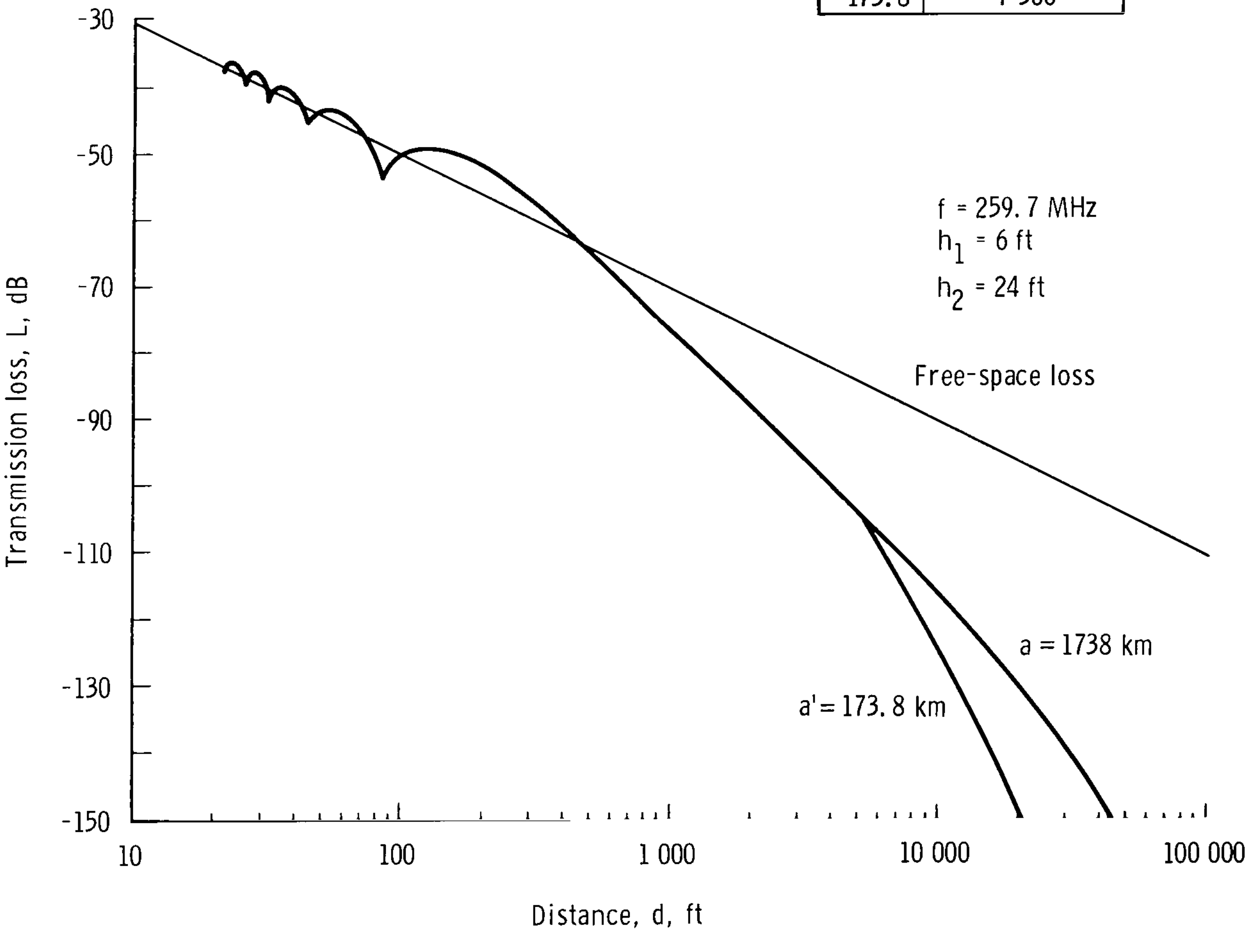

(b) Transmission loss for astronaut-to-lunar-module link.

Figure 7. - Small-hill effects.

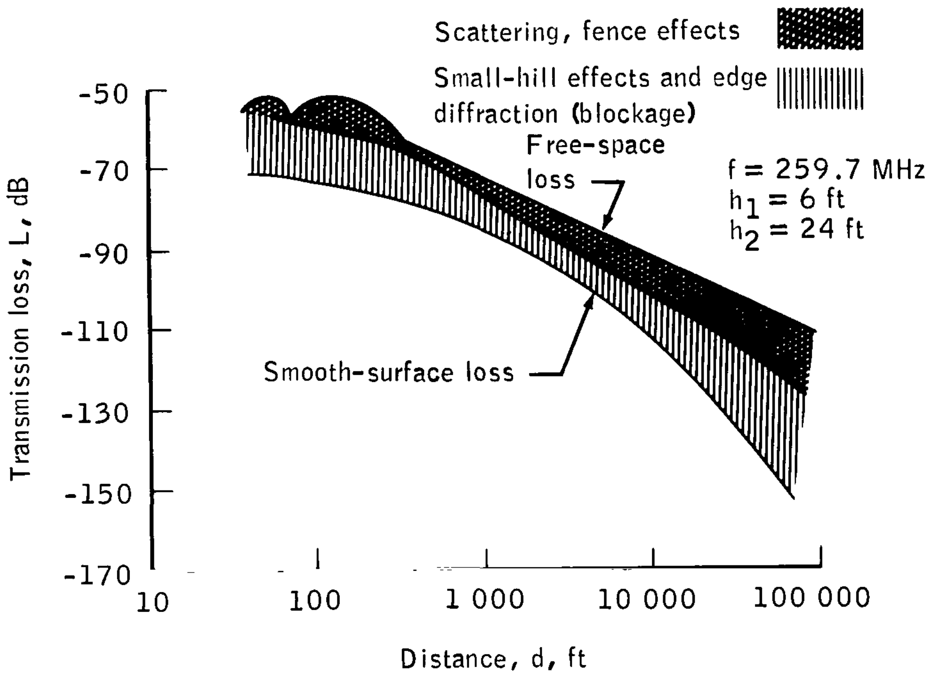

Figure 8. - Combined effects for the curved-surface model and roughness effects for the astronaut-to-lunar-module link.

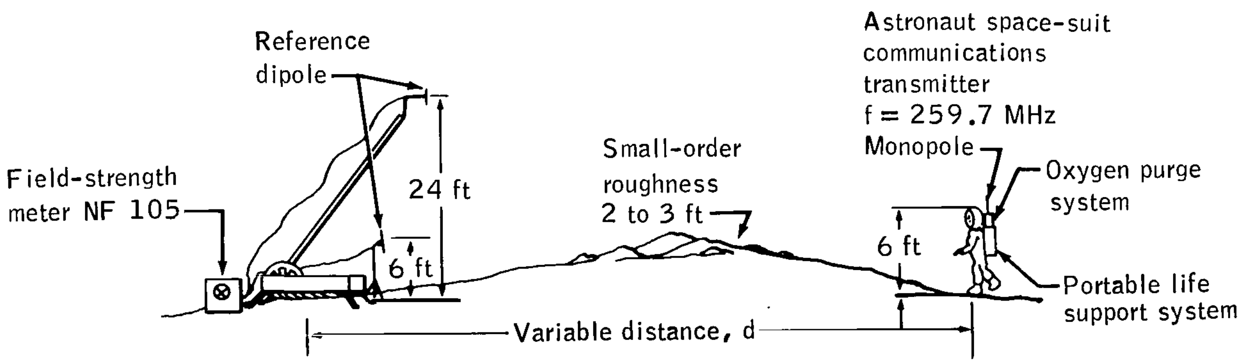

Figure 9. - Test setup.

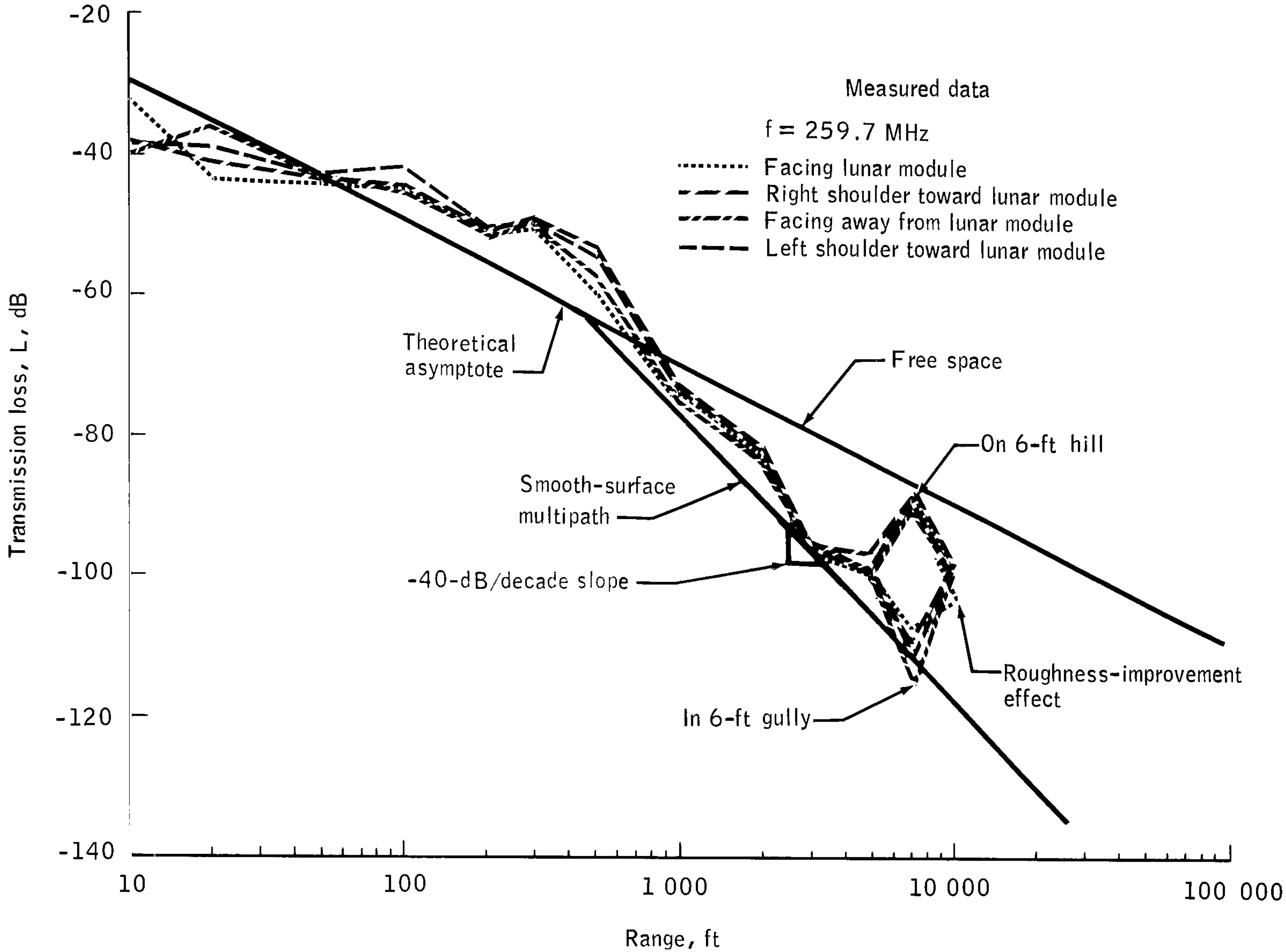

Figure 10. - Astronaut-to-lunar-module link with astronaut standing.

NASA-Langley, [illegible] — 7 S-195

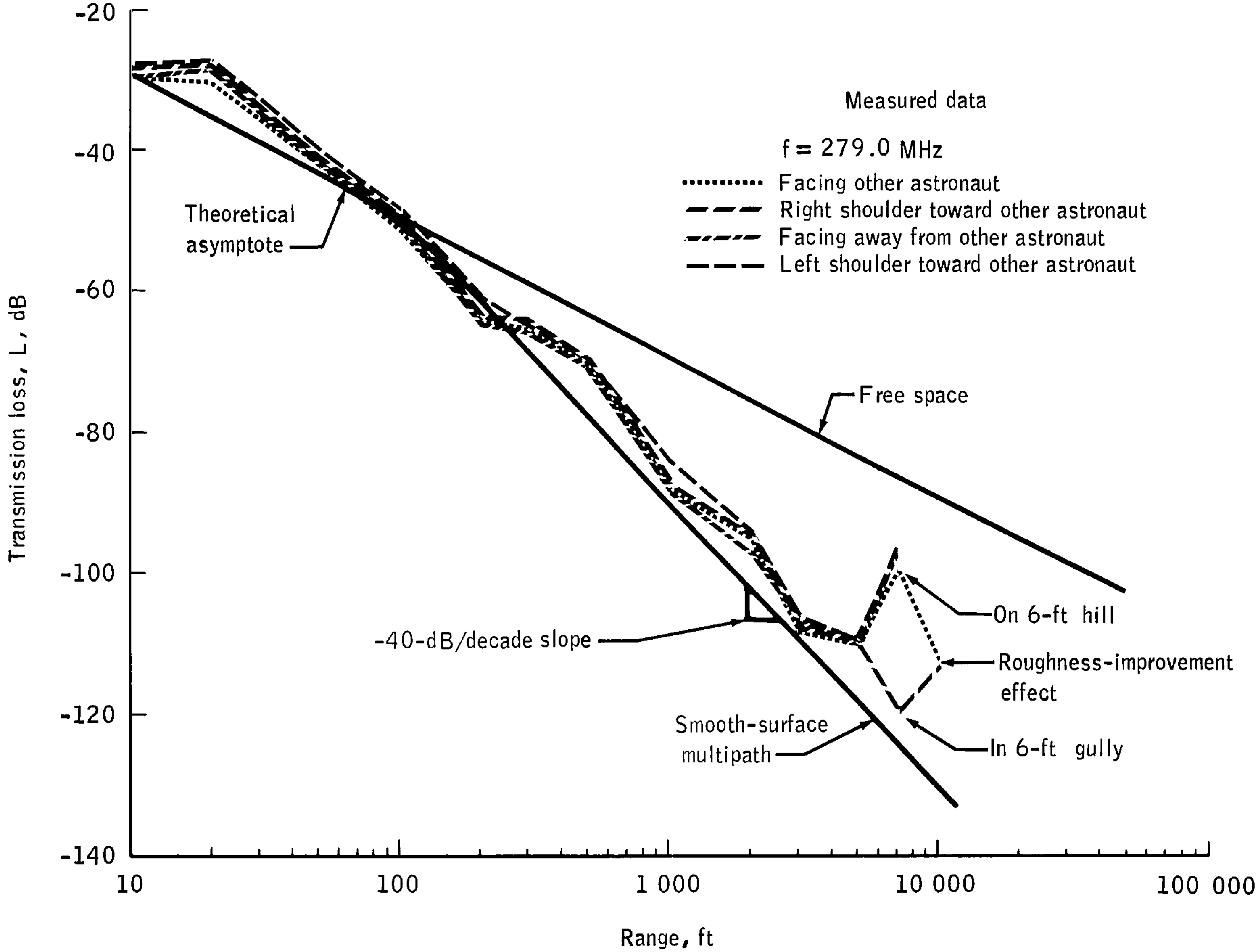

Figure 11. - Astronaut-to-astronaut link with astronaut standing.

NATIONAL AERONAUTICS AND SPACE ADMINISTRATION
WASHINGTON, D. C. 20546

OFFICIAL BUSINESS

FIRST CLASS MAIL

POSTAGE AND FEES PAID
NATIONAL AERONAUTICS AND
SPACE ADMINISTRATION

[illegible]

POSTMASTER: If Undeliverable (Section 158 Postal Manual) Do Not Return

"The aeronautical and space activities of the United States shall be conducted so as to contribute . . . to the expansion of human knowledge of phenomena in the atmosphere and space. The Administration shall provide for the widest practicable and appropriate dissemination of information concerning its activities and the results thereof."

—NATIONAL AERONAUTICS AND SPACE ACT OF 1958

NASA SCIENTIFIC AND TECHNICAL PUBLICATIONS

TECHNICAL REPORTS: Scientific and technical information considered important, complete, and a lasting contribution to existing knowledge.

TECHNICAL NOTES: Information less broad in scope but nevertheless of importance as a contribution to existing knowledge.

TECHNICAL MEMORANDUMS: Information receiving limited distribution because of preliminary data, security classification, or other reasons.

CONTRACTOR REPORTS: Scientific and technical information generated under a NASA contract or grant and considered an important contribution to existing knowledge.

TECHNICAL TRANSLATIONS: Information published in a foreign language considered to merit NASA distribution in English.

SPECIAL PUBLICATIONS: Information derived from or of value to NASA activities. Publications include conference proceedings, monographs, data compilations, handbooks, sourcebooks, and special bibliographies.

TECHNOLOGY UTILIZATION PUBLICATIONS: Information on technology used by NASA that may be of particular interest in commercial and other non-aerospace applications. Publications include Tech Briefs, Technology Utilization Reports and Notes, and Technology Surveys.

Details on the availability of these publications may be obtained from:

SCIENTIFIC AND TECHNICAL INFORMATION DIVISION

NATIONAL AERONAUTICS AND SPACE ADMINISTRATION

Washington, D.C. 20546